Published online 11 April 2017

Nucleic Acids Research, 2017, Vol. 45, No. 11 ***6837–6847***
doi: 10.1093/nar/gkx254

Stepwise assembly of the earliest precursors of large ribosomal subunits in yeast

Wu Chen[1,2,3], Zhensheng Xie[4,5], Fuquan Yang[4,5] and Keqiong Ye[3,5,*]

[1]College of Biological Sciences, China Agricultural University, Beijing 100193, China, [2]National Institute of Biological Sciences, Beijing 102206, China, [3]Key Laboratory of RNA Biology, CAS Center for Excellence in Biomacromolecules, Institute of Biophysics, Chinese Academy of Sciences, Beijing 100101, China, [4]Laboratory of Proteomics, Institute of Biophysics, Chinese Academy of Sciences, Beijing 100101, China and [5]University of Chinese Academy of Sciences, Beijing 100049, China

Received January 19, 2017; Revised April 01, 2017; Editorial Decision April 03, 2017; Accepted April 04, 2017

ABSTRACT

Small ribosomal subunits are co-transcriptionally assembled on the nascent precursor rRNA in *Saccharomyces cerevisiae*. It is unknown how the highly intertwined structure of 60S large ribosomal subunits is initially formed. Here, we affinity purified and analyzed a series of pre-60S particles assembled *in vivo* on plasmid-encoded pre-rRNA fragments of increasing lengths, revealing a spatiotemporal assembly map for 34 trans-acting assembly factors (AFs), 30 ribosomal proteins and 5S rRNA. The gradual association of AFs and ribosomal proteins with the pre-rRNA fragments strongly supports that the pre-60S is co-transcriptionally, rather than post-transcriptionally, assembled. The internal and external transcribed spacers ITS1, ITS2 and 3′ ETS in pre-rRNA must be processed in pre-60S. We show that the processing machineries for ITS1 and ITS2 are primarily recruited by the 5′ and 3′ halves of pre-27S RNA, respectively. Nevertheless, processing of both ITS1 and ITS2 requires a complete 25S region. The 3′ ETS plays a minor role in ribosome assembly, but is important for efficient rRNA processing and ribosome maturation. We also identified a distinct pre-60S state occurring before ITS2 processing. Our data reveal the elusive co-transcriptional assembly pathway of large ribosomal subunit.

INTRODUCTION

The ribosome is a large two-subunit RNA–protein complex responsible for protein translation in all organisms. In *Saccharomyces cerevisiae*, the 40S small subunit (SSU) is composed of 18S rRNA and 33 SSU r-proteins (RPSs) and the 60S large subunit (LSU) contains 25S, 5.8S and 5S rRNAs and 46 LSU r-proteins (RPLs). Ribosome assembly is a complicated and dynamic process that requires transcription, modification and processing of rRNAs and association of ribosomal proteins (1,2). More than 200 protein assembly factors (AFs) and numerous small nucleolar RNAs (snoRNAs) function in ribosome assembly. Each subunit matures by forming a series of pre-ribosomal particles that transit from the nucleolus through the nucleoplasm to the cytoplasm.

The 18S, 5.8S and 25S rRNAs are co-transcribed as a long 35S precursor rRNA (pre-rRNA) that additionally contains four external and internal transcribed spacers (ETS and ITS). Electron microscopy images of rDNA chromatin spreads have visualized the early assembly process of ribosomes on the nascent pre-rRNA. The 5′ growing end of the pre-rRNA transcript is progressively packed into a large knot, which is the earliest precursor of SSU known as the 90S pre-ribosome or SSU processome (3–6). After cleavage of the pre-rRNA at sites A0, A1 and A2, 90S is transformed into a pre-40S ribosomal particle, which is rapidly exported to the cytoplasm for final maturation. Although the co-transcriptional assembly process of the SSU is well established (5,7,8), whether the LSU is assembled co-transcriptionally is less evident. The 90S particle can be cleaved off co-transcriptionally under favorable growth conditions. New terminal knot structures, indicative of nascent pre-60S particles, were only occasionally observed on the remnant transcript harboring 5.8S and 25S rRNAs (5). The SSU is composed of four structurally distinct domains, whereas the LSU is a monolithic structure with six highly intertwined domains. This feature raises a major question as to whether the LSU assembles post-transcriptionally in a cooperative manner on the full length pre-rRNA.

The pre-rRNA is released from chromatin by Rnt1-mediated cleavage of 3′ ETS (9,10). After the ITS1 is processed in the nucleolus, the pre-60S particle undergoes a large compositional change and a C2 cleavage of ITS2 at around the time of transition to the nucleoplasm. Further

*To whom correspondence should be addressed. Tel: +86 10 64887672; Fax: +86 10 64887672; Email: yekeqiong@ibp.ac.cn

maturation in the nucleoplasm proceeds through several distinct states, some of which have recently been analyzed by cryo-EM. An early nucleoplasmic particle displays two prominent structural features: a 180°-rotated 5S ribonucleoprotein (RNP) composed of 5S RNA, L5 and L11 bound at the central protuberance (CP), as well as a foot structure assembled on the partially processed ITS2 (11,12). A middle nucleoplasmic state is characterized by the association of Sda1, the Rix1-Ipi1-Ipi2 complex and Rea1/Mdn1, an almost mature CP structure and the disappearance of ITS2 and the foot structure (11,13). At the late stage, the pre-60S particle becomes competent for export after release of Nog2 and other AFs (14). The release of Nog2 allows for recruitment of the export factor Nmd3. In the cytoplasm, the 60S subunit eventually matures after dissociation of all remaining AFs and assembly of 10 late-binding RPLs (15–17).

The pre-60S maturation at the nucleoplasmic and cytoplasmic stage has been described in great detail, but how the earliest pre-60S is formed remains unknown. Recently, analysis of the composition of RNPs assembled on a series of pre-18S fragments has allowed the determination of a stepwise and dynamic assembly map for the 90S pre-ribosome (7,8). In this study, we applied a similar approach to determine the assembly order of the earliest pre-60S particles. We find that the pre-60S is formed in a stepwise manner on the pre-rRNA transcripts of increasing length, providing strong evidence for its co-transcriptional assembly.

MATERIALS AND METHODS

Plasmids

The pWL109 (URA3 marker) plasmid encoding the 35S rDNA sequence between a GAL7 promoter and a terminator was kindly provided by Dr Skip Fournier (18). The rDNA sequence between nucleotide 1 of 5′ ETS and nucleotide 246 of ITS1 were removed by QuikChange site-directed mutagenesis. Four copies of MS2 coat protein binding motif (MS2-tag) were assembled by overlapping oligonucleotides, cloned into a pEASY-T vector and confirmed by DNA sequencing. The MS2-tag was PCR-amplified and cloned into the modified pWL109 plasmid between nucleotides 214 and 215 of ITS2 by using the transfer-PCR approach (19). In addition, a labeling sequence (5′- CTGGTAGGAAGCTGCAGCC-3′) was inserted between nucleotides 142 and 143 of 25S rRNA by the QuikChange approach (18). The resultant plasmid was named pLM430. The 3′ truncations ending at nucleotides 635, 1448, 1878, 2358, 2994 or 3396 of 25S were constructed by removal of the unneeded sequences from pLM430 with QuikChange and appropriate primers.

Purification of pre-60S particles

The fusion of maltose-binding protein (MBP) and MS2 coat protein (MBP-MS2) was prepared, and the resultant protein was loaded onto amylose beads (NEB), as previously described (7). Yeast cells were manipulated according to standard protocols. Unless specifically mentioned, yeast cells were grown in YPD (1% yeast extract, 2% peptone, 0.003% adenine and 2% glucose) medium at 30°C. Tandem affinity purification (TAP)-tagged Nop7/BY4741 strain (MATa, his3Δ1, leu2Δ0, met15Δ0, ura3Δ0, Nop7-TAP::HIS3MX6) was purchased from Open Biosystems. The Nop7-TAP strain was transformed with an rDNA plasmid and selected on Ura-deficient Synthetic Complete (SC) medium. A single clone was propagated in Ura-deficient SC medium containing 2% galactose as the sole carbon source. The cells were further cultured in 6 liter YPG medium (1% yeast extract, 2% peptone, 0.003% adenine and 2% galactose) until OD600 = 1. The yeast cells were collected, washed with water and stored at −80°C before use.

All purification steps were conducted at 4°C or on ice. Yeast cells were resuspended in 10 ml of lysis buffer (50 mM HEPES, pH 7.4, 200 mM KCl, 1 mM ethylenediaminetetraacetic acid (EDTA), 1 mM dithiothreitol (DTT)), frozen in liquid nitrogen and disrupted with a tissue lyser. After centrifugation at 20 000 *g* for 40 min, the supernatant was collected and incubated with 500 μl of MBP-MS2 protein-loaded amylose beads for 1.5 h. The beads were washed with 100 ml of lysis buffer and eluted with 1 ml of elution buffer (50 mM HEPES, pH 7.4, 200 mM KCl, 1 mM EDTA, 2 mM DTT, 10 mM maltose). The eluate was incubated with 15 mg IgG-coated Dynabeads (Invitrogen) in 2 ml of RNP buffer (20 mM HEPES, pH 7.4, 110 mM KOAc, 40 mM NaCl) for 0.5 h. The beads were washed with 5 ml of RNP buffer and cleaved with 10 μg Tobacco Etch Virus (TEV) protease in 1 ml RNP buffer to release the RNP.

The Ssf1-TAP, Nop7-TAP, Rix1-TAP and Arx1-TAP strains (BY4741 background) were purchased from Open Biosystems. The chromosomal pre-60S particles were purified with IgG-coated Dynabeads and released by TEV cleavage.

Mass spectrometric analysis

Samples of plasmid-derived particles were precipitated with 10% trichloroacetic acid, resolved briefly by SDS-PAGE and visualized by silver staining. The gels were excised into three to four pieces for each lane, washed twice with water and destained with a freshly prepared solution of 15 mM $K_3Fe(CN)_6$ and 50 mM $Na_2S_2O_3$. Gel pieces were dehydrated with 100% acetonitrile and dried for 5 min in a SpeedVac. Disulfide bonds were reduced with 10 mM DTT for 45 min at 56°C, and free sulfhydryl groups were alkylated with 55 mM iodoacetamide for 60 min at 25°C in the dark. Gel pieces were sequentially washed with 50 mM NH_4HCO_3 and 50% acetonitrile/50 mM NH_4HCO_3 and then dehydrated with 100% acetonitrile. After being dried with a SpeedVac, the gel was rehydrated in 100 ng/μl trypsin and 50 mM NH_4HCO_3 (pH 8.3) on ice for 30 min. The digestion was carried out at 37°C for 60 min and then quenched with 1.0% formic acid. The tryptic peptides were extracted twice with 60% acetonitrile containing 0.1% formic acid, and the combined digest solution was concentrated to 25 μl under vacuum.

The digested peptides were analyzed on a nanoLC-LTQ-Orbitrap XL mass spectrometer (Thermo, San Jose, CA, USA) at a resolution of 60 000. nanoLC was conducted with an Eksigent naloLC 1D plus system equipped with ReproSil-Pur C18-AQ (Dr Maisch GmbH, Ammerbuch) trapping columns (packed in-house, i.d. 150 μm; length 30 mm; resin, 5 μm) and ReproSil-PurC18-AQ (Dr Maisch

GmbH, Ammerbuch) analytical columns (packed in-house, i.d., 75 μm; length 150 mm; resin, 3 μm). Solvents used were 0.5% formic acid water solution (buffer A) and 0.5% formic acid acetonitrile solution (buffer B). Trapping was performed with buffer A at 2 μl/min for 15 min. The peptides were eluted with a gradient of 4% B at the first 4 min, 4–10% B in 3 min, 10–36% B in 75 min, 36–80% B in 5 min, 80% B for 7 min, 80–4% in 1 min and 4% B hold for 9 min to equilibrate at a flow rate of 300 nl/min. Eluted peptide cations were converted to gas-phase ions with a Nanospray Flex ion source at 2.1 kV. The mass spectrometer was operated in data-dependent mode to automatically switch between MS and MS/MS. Survey full scan MS spectra were acquired from m/z = 300 to 1800. The 10 most intense ions with >2 charge state and >500 intensity were fragmented in a linear ion trap using with normalized collision energy of 35%. For the Orbitrap, the AGC target value was set to 1e6, and the maximum fill time for full MS was set to 500 ms. Fragment ion spectra were acquired in the LTQ with an AGC target value of 3e4 and a maximum fill time of 150 ms. Dynamic exclusion for selected precursor ions was set at 120 s. The lock mass option was enabled for the 445.120025 ion.

The raw data were processed using Proteome Discoverer (version 1.4.0.288, Thermo Fischer Scientific). MS2 spectra were searched with the SEQUEST engine against the yeast UniProt database. A database search was performed with the following parameters: precursor mass tolerance, 20 ppm; MS/MS mass tolerance, 0.6 Da; two missed cleavage sites allowed for tryptic peptides; methionine oxidation and protein N-terminal acetylation as variable modifications; carbamidomethyl as fixed modification. Peptide spectral matches were validated with a targeted decoy database search at 1% false discovery rate with Percolator. Peptide identifications were grouped into proteins according to the law of parsimony.

The samples of chromosomal pre-60S were analyzed with an LTQ mass spectrometer, as previously described (7). Protein quantification by spectral counts and treatment of duplicated r-proteins were conducted as previously described (7).

Northern blot

Total RNA extraction and northern blot analysis were performed as previously described (7). Plasmid-derived particles were purified from 6 liters of yeast cells via MS2-tag and Nop7-TAP. The RNA in purified pre-60S particles was extracted from beads with TRIzol. For large RNA analysis, RNA was separated on 1.2% agarose-formaldehyde gels. The following DNA probes were used for hybridization: 25S-tag: 5′-GGGCAGGCTGCAGCTTCCTACCAG-3′; A2-A3: 5′-ATGAAAACTCCACAGTG-3′; C2-C1: 5′-AGATTAGCCGCAGTTGG-3′; A3-B: 5′-CCAGTTACGAAAATTCTTG-3′; E-C2: 5′-TGAGAAGGAAATGACGCT-3′; 5S: 5′-CTACTCGGTCAGGCTC-3′.

Primer extension

Primer extension was conducted with Avian Myeloblastosis Virus (AMV) reverse transcriptase (Promega) mainly following the manufacturer's protocol. Total RNA (7 μg) was mixed with ∼1.5 pmol 5′-^{32}P-labeled 25S-tag primer, 5 μl Primer Extension 2 × Buffer (100 mM Tris–HCl pH 8.3, 100 mM KCl, 20 mM $MgCl_2$, 20 mM DTT, 2 mM each dNTP, 1 mM spermidine) and water to 11 μl volume. Primer annealing was conducted at 75°C for 5 min and then at 65°C for 1 h. The mixture was added with 1 μl (10 U) AMV reverse transcriptase, 1.4 μl pre-warmed sodium pyrophosphate (40 mM), 1.6 μl water and 5 μl Primer Extension 2 × Buffer and incubated at 42°C for 30 min. Sequencing ladders were prepared using the Sanger dideoxy method on plasmid pLM430. DNA was resolved in an 8% polyacrylamide/8M urea sequencing gel. The gel was dried and visualized by autoradiography.

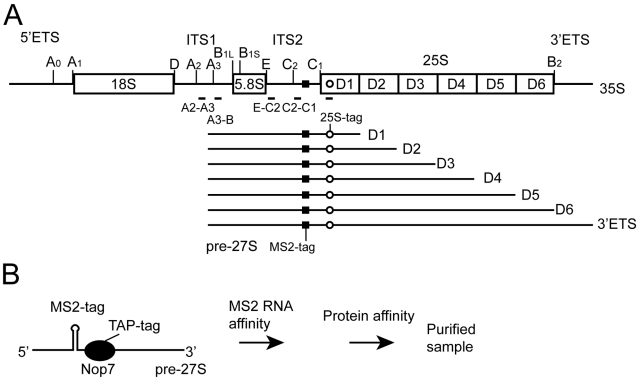

Figure 1. Purification of plasmid-derived pre-60S particles. (**A**) Construction of pre-27S RNA fragments. The structural diagram and processing sites of 35S pre-rRNA are shown on the top. Seven pre-27S RNA fragments terminate after one of six domains I–VI (D1–D6) of 25S rRNA or the 3′ ETS and contain an MS2-tag (square) in ITS2 and a plasmid-specific sequence (circle, 25S-tag) in domain I. These RNAs are transcribed under a *GAL*-promoter in multiple-copy 2μ plasmids. Locations of hybridization probes are indicated. (**B**) Plasmid-derived pre-60S particles were affinity purified via an MS2-tag in pre-rRNA and then via TAP-tagged Nop7.

RESULTS

Purification and analysis of progressively assembled pre-60S particles

To determine the order by which AFs and RPLs assemble into the earliest pre-60S particle, we expressed through plasmid in yeast a series of pre-27S rRNA fragments starting at a position between sites A2 and A3 and terminating after one of six domains I–VI (D1–D6) of 25S rRNA or the natural end of the 3′ ETS and purified the *in vivo* assembled RNPs (Figure 1A). These complexes mimicked the assembly intermediates formed on the nascent pre-rRNAs and provided snapshots of the co-transcriptional assembly process of pre-60S. The longest transcript resembles the 27SA2 product of A2 cleavage of 35S pre-rRNA and can be processed and assembled into functional 60S subunits (18). For convenience, these RNAs are referred to by their ending domains.

To facilitate affinity purification, four copies of MS2-tag were inserted in a middle position of ITS2. The MS2-tag did not interfere with the rRNA processing, because the full-length pre-27S could be processed into 25S rRNA with a

normal 5′-end (Figure 2A, lane 1 and Supplementary Figure S2). These RNAs were expressed in a yeast strain in which Nop7, an AF associated with nucleolar and nucleoplasmic pre-60S particles (20), was fused to a C-terminal TAP-tag (21). The *in vivo* assembled RNPs were affinity purified first via the MS2-tag on the RNA and then via the TAP-tag on the protein (Figure 1B).

The purified RNPs were analyzed by northern blotting to identify associated RNAs (Figure 2) and by mass spectrometry to identify associated proteins (Figures 3 and 4; Supplementary Data Set 1). Mass spectrometry analyses were duplicated for two independently purified samples. The total spectral counts per 100 residues (SCPHR) were calculated for each identified protein as a semi-quantitative indicator of absolute molar amount (7). The SCPHR was further normalized against a set of stably associated reference proteins to obtain the relative spectral abundance factor (RSAF). The RSAF value indicates stoichiometry relative to the reference proteins and allowed for comparison of protein abundance within and across samples. The known pre-60S AFs and RPLs constituted 65.4–83.9% of all identified proteins in terms of molar amount, demonstrating high purity of our samples. Majority of identified AFs displayed specific binding pattern as a function of RNA length. An AF was deemed to be associated if its RSAF value was >0.1 in at least one sample. A few AFs with very weak association or random binding patterns were not assigned (Supplementary Data Set 1).

For comparison with plasmid-derived particles, we also purified chromosome-derived pre-60S particles via TAP-tagged Ssf1, Nop7, Rix1 and Arx1 (Figure 3A and Supplementary Data Set 1). These proteins associate with pre-60S for different durations (Figure 3B). Ssf1 is present only in the nucleolar particles (22). Nop7 associates with both nucleolar and nucleoplasmic particles (20). Rix1 is bound only at the middle nucleoplasmic stage (13,20,23). Arx1 enters the pre-60S particle at the early nucleoplasmic stage and dissociates in the cytoplasm (12,20,24).

Processing of plasmid-derived pre-27S RNA

The 27SA pre-rRNA is processed into 5.8S and 25S rRNAs by removal of ITS1 and 3′ ETS, yielding 27SB pre-rRNA and subsequent cleavage and processing of ITS2 (Supplementary Figure S1). We performed northern blotting to assess whether the plasmid-derived pre-27S RNA fragments could be processed in yeast. The RNAs from plasmid were detected by a plasmid-specific sequence inserted in domain I (Figure 1A). The complete pre-27S transcript was processed into 25S rRNA, which strongly accumulated in yeast (Figure 2A, lane 1), as previously reported (18). Removal of the 3′ ETS in the D6 RNA had no effect on the abundance of the precursor transcript, but strongly reduced the yield of 25S rRNA, indicating that 3′ ETS is important for processing efficiency (Figure 2A, lane 2). The D5 and shorter transcripts each exhibited a single major species, indicating that they cannot be processed at the ITS2 region (Figure 2A, lanes 3–7). We concluded, within the current length resolution, that a complete 25S region is required for ITS2 processing.

We also analyzed RNA species in the purified particles (Figure 2B–N). These RNAs showed substantial degradation after two steps of prolonged purification, but the intact pre-27S species were still detectable. Although the D6 and 3′ ETS RNA can be processed at ITS2 (Figure 2A), the D6 and 3′ ETS particles contained minimal amounts of 7S pre-rRNA, a product of C2 cleavage (Figure 2M, lanes 3–4). As a comparison, the Ssf1-TAP and Nop7-TAP particles contained substantial amounts of 7S intermediate (Figure 2M, lanes 5–6). Our purification strategy used an MS2-tag placed at the ITS2 region and apparently enriched for RNA species with an intact ITS2.

The 5S rRNA is transcribed from separate genes and probably assembles into pre-60S at an early stage (25). Northern blot analysis showed that the 5S rRNA is assembled until the entire 25S region is present (Figure 2E and N). Notably, the D6 and 3' ETS particles contain substoichiometic amounts of 5S rRNA relative to 27S pre-rRNA, as compared to the chromosomal Ssf1-TAP or Nop7-TAP particles (Figure 2K and N). This suggests that 5S rRNA is weakly associated to the D6 and 3' ETS particles.

The products of ITS1 processing cannot be resolved by size and hence were differentiated by ITS1-targeting probes. Each of the D1 to D5 RNAs with an incomplete 25S region showed comparable intensity when it was hybridized to probes targeting ITS1, 25S or ITS2 (Figure 2B–H, lanes 4–8), indicating that ITS1 was not processed in these RNAs. In contrast, the top species of D6 and 3′ ETS RNAs showed significantly weaker intensities when they were hybridized to probes targeting ITS1 compared with probes targeting 25S and ITS2 (Figure 2B–H, lanes 2–3; Figure 2J–L, lanes 3–4), indicating that ITS1 was partially processed in these RNAs. The quantification results showed that the 3′ ETS particle contained a higher percentage of ITS1-processed RNA (∼70%) compared with the D6 particle (∼50%) (Figure 2I). We concluded that ITS1 processing also requires the presence of complete 25S rRNA.

Assembly of ribosomal proteins

The mass spectrometry signals were noisier for RPLs than AFs, making the assignment of assembly point less certain for some RPLs. Among 46 RPLs, 10 are known to assemble at the cytoplasm (2) and are generally of low abundance in the purified particles. The remaining RPLs are associated with the early nucleoplasmic particle (11,12) and most likely also present in the fully assembled D6 and 3′ ETS particles. We tentatively assigned assembly point for 30 RPLs, considering their background level, change as a function of RNA length and reproducibility in two analyzed samples (Figure 4A and B). It is noteworthy that the assembly order of ribosomal proteins cannot be determined previously for the 90S particles due to noisy signals (7,8).

The assembly points of RPLs are generally consistent their primary binding sites on 25S rRNA. Some RPLs, many of which bound at the D6 step, show delayed binding, suggesting that their association is dependent on the global structure of 60S. L27 and L14 primarily bind at domain III and VI, respectively and their strong binding signals to the D2 fragment may be non-specific.

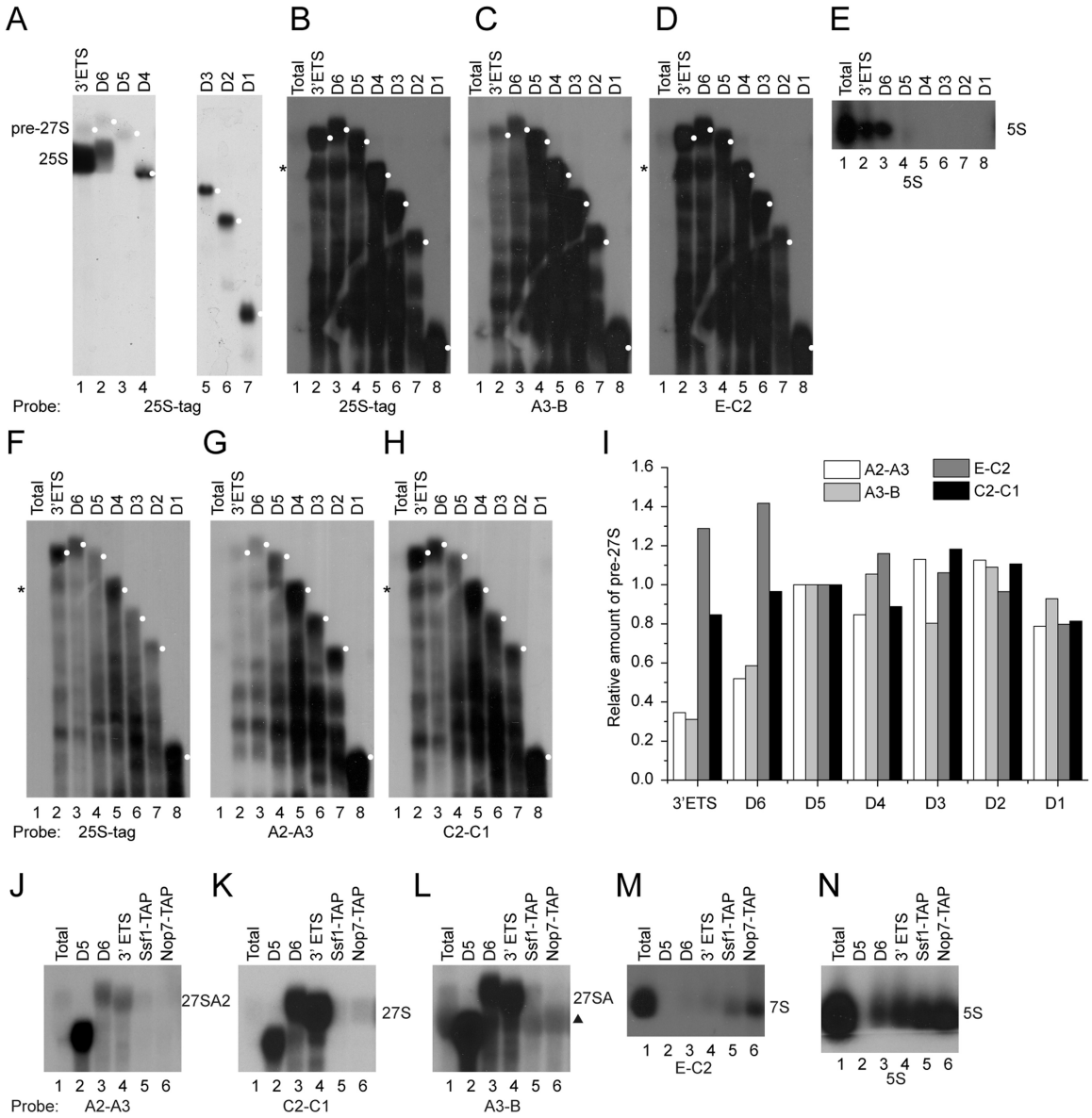

Figure 2. Processing of plasmid-derived pre-27S RNAs. (**A**) Total RNAs from Nop7-TAP strains that expressed an indicated pre-27S RNA fragment were separated on agarose-formaldehyde gels and blotted with ^{32}P-labeled oligonucleotides that hybridize to the plasmid-specific 25S-tag in the D1 domain. The longest pre-27S RNAs in each lane are labeled with white circles. (**B**–**H**) Northern blot analysis of RNAs in purified pre-60S particles. Total RNA (15 μg) in the first lane was from the BY4741 strain. RNAs were separated on two gels (B–E and F–H) and hybridized to probes 25S-tag (B and F), A3-B(C), E-C1(D), 5S (E), A2-A3(G) and C1-C2 (H). The binding sites of probes are indicated in Figure 1A. The top bands labeled with white circles represent species containing an intact ITS2. Asterisk indicates a degradation product that had a similar size as 25S rRNA and hybridized to the ITS2-targeting probes. (**I**) Quantification of the top RNA species detected by different probes in B–D and F–H. The volume of the top band in each lane detected by a probe was divided by the volume detected by 25S-tag. The resultant ratios were further normalized to that of D5 RNA. (**J**–**N**) Northern blot analysis of RNA in the D5, D6 and 3′ ETS particles and the chromosomal Ssf1-TAP and Nop7-TAP particles. Triangles indicate cross-hybridization signals of 25S rRNA.

Stepwise assembly of pre-60S

The D1 transcript encompassing part of ITS1, 5.8S rRNA, ITS2 and domain I of 25S rRNA was found to associate with 15 AFs (Figure 3A). L8 and L15 were also consistently enriched in the two analyzed samples. Among the associated proteins, some have been shown to form subcomplexes: Rrp5, Noc2 and Mak21/Noc1 (26); Pwp1, Nop12, Brx1, Ebp2, L8 and L15 (27,28); Brx1 and Ebp2 (29); and Erb1, Ytm1 and Nop7 (27,30–32). Our data show that these factors co-assemble to the D1 RNA at the earliest stage of pre-60S formation. The binding of these proteins is also supported by available structural information. Nop12, Erb1, Cic1, Nop15 and Rlp7 crosslink at the 5.8S, ITS2 and D1 regions (33,34) and Rrp5 crosslinks at the ITS1 region (35). In the structure of fully assembled pre-60S, L8 and L15 extensively interact with the 5.8S/D1 domain, and Nop7, Cic1, Rlp7 and Nop15 bind at the ITS2 region (11,12). Our data

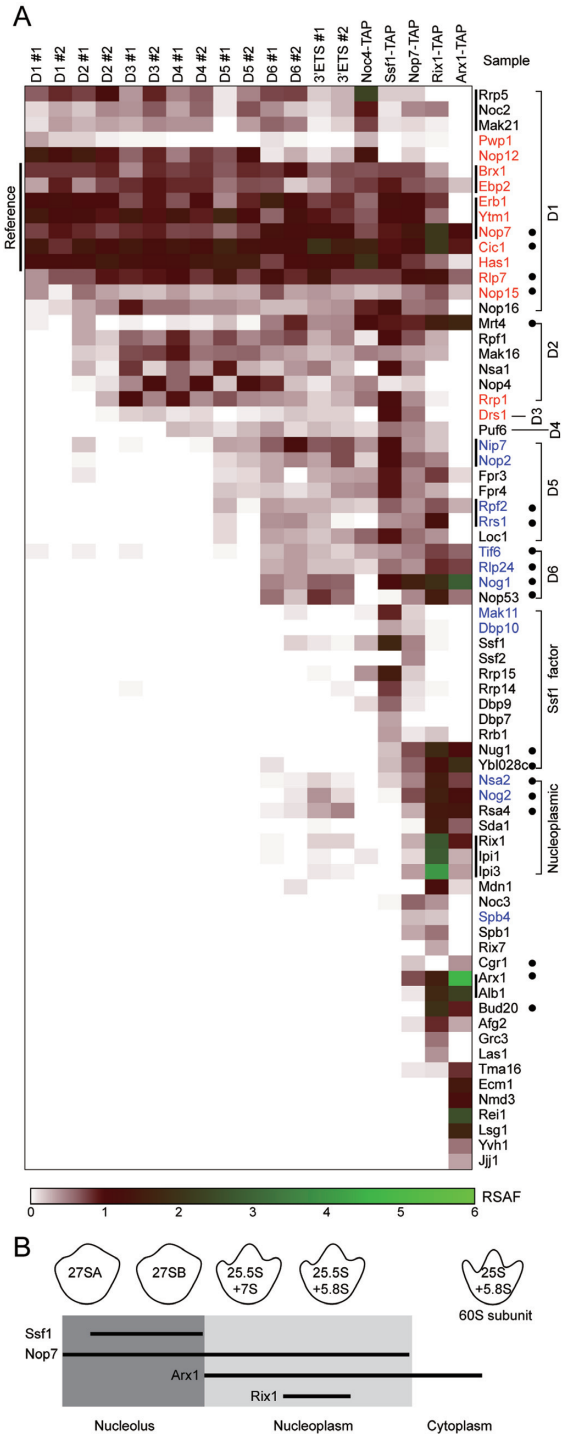

Figure 3. Assembly order of AFs to pre-60S. (**A**) Heatmap of AFs associated with progressively elongated pre-27S RNAs and chromosomal pre-60S particles. The proteins are color-coded according to their RSAF values normalized against the reference proteins Brx1, Ebp2, Erb1, Ytm1, Nop7, Cic1 and Has1 by default. The Arx1-TAP particle is normalized against Nop7 and Cic1 because the other reference proteins were of very low abundance or absent. The plasmid-derived particles were purified and analyzed in duplicate. Noc4-TAP, Ssf1-TAP, Rix1-TAP and Arx1-TAP are chromosomal particles. A3-factors and B-factors are colored red and blue, respectively. Solid circles mark 19 AFs found in the structure of an early nucleoplasmic pre-60S (11,12). (**B**) Association duration of the indicated AFs with evolving pre-60S particles. Pre-rRNA species in different pre-60S particles are shown.

demonstrate that these factors can form a stable subcomplex with the D1 pre-rRNA fragment independently of the rest of pre-60S structure.

The addition of domain II resulted in the recruitment of ~6 AFs (Mrt4, Rpf1, Mak16, Nsa1, Nop4 and Rrp1). Mrt4 is a homolog of the r-protein P0 and binds at helices 42–44 of domain II (11,12). The amount of Mrt4 fluctuated in the D2–D5 particles, suggesting that it was weakly bound to these partially assembled particles. The binding of Nop4 was consistent with its crosslinking to multiple sites in domains II and III (34).

The presence of domain III induced the appearance of Drs1 and additionally strengthened the association of most D2-dependent AFs. The addition of domain IV led to the association of Puf6. Puf6 is an atypical Pumilio-repeat protein that appears to bind to double-stranded RNA structures (36).

The inclusion of domain V resulted in the detection of Nop2, Nip7, Rpf2, Rrs1, Loc1, Fpr3 and Fpr4 and significant enrichment of L1. Some of these associated proteins appear to directly interact with domain V. Nop2 is the methyltransferase for C2870 in domain V (37) and is apparently recruited by its substrate sequence. Nip7 may co-assemble with Nop2 since they form a stable subcomplex (38). L1 binds helices 77 and 78 in domain V, forming the L1 stalk. The Rpf2–Rrs1 complex binds at the base of the CP, which is composed of helices 81–87 in domain V and the 5S RNP (12,39–41).

Fully assembled pre-60S particles

The completion of 25S rRNA in the D6 transcript led to the association of Tif6, Rlp24, Nog1, Nop53 and 5S rRNA (Figures 2E, N and 3). Tif6, Rlp24 and Nog1 are positioned at an arc region extended from the CP to the exit tunnel and contact domain VI and L3 and L23 (11,12), accounting for their D6-dependent association. Nop53 binds at the foot structure around the ITS2 (11) and serves as an anchoring site for Mtr4, which recruits the exosome for processing of 7S pre-rRNA (42–45). The presence of Nop53 in the D6 particle, which contains an intact ITS2, suggests that Nop53 is already recruited before C2 cleavage.

The 3′ ETS particle had a very similar protein profile to that of the D6 particle, but was more enriched in a few late-associating AFs. These AFs include Nsa2, Nog2 and Rsa4 (RSAF = 0.2–0.4), which associate at the early nucleoplasmic stage (11,12), as well as Sda1, Rix1, Ipi1 and Ipi3 (RSAF = ~0.1), which are specifically present at the middle nucleoplasmic state (11,13). The D6 particle contained only minimal amounts of these late-associating AFs (RSAF < 0.1), indicating that it is less evolved. The appearance of these late-binding AFs demonstrated that a fraction of the purified particles had evolved into late stages. This is possible because the D6 and 3′ ETS transcripts are competent for pre-rRNA processing (Figure 2). In addition, the bait protein Nop7 used in the second step of purification binds pre-60S for an extended time (Figure 3A and B). The 3′ ETS particle was largely depleted of the Rrp5/Noc2/Mak21 complex (Figure 3A), which is specifically associated with early pre-60S particles (26,46).

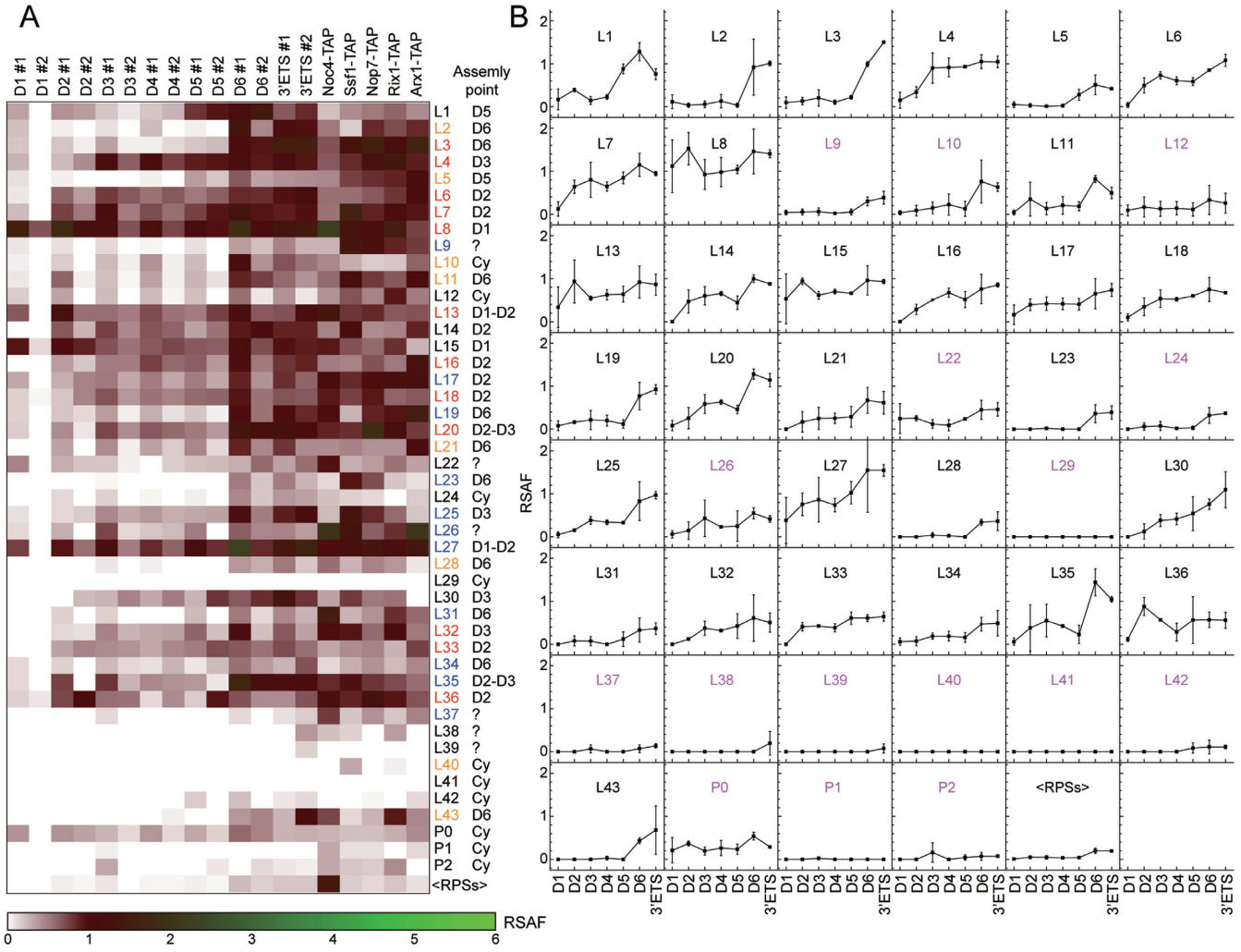

Figure 4. Assembly order of PRLs. (**A**) Heatmap of RPLs in pre-60S particles. The proteins are color-coded according to their RSAF values normalized against Brx1, Ebp2, Erb1, Ytm1, Nop7, Cic1 and Has1 for plasmid-derived particles. The total RSAF value of RPLs of chromosomal particles is further normalized against that of the 3′ ETS #1 particle. The last row shows average RSAFs for RPSs. The early, middle, late and other unclassified RPLs are colored red, blue, orange and black, respectively. The deduced assembly points or ranges are displayed on the right. Cy indicates cytoplasmic assembly, and question mark denotes 'not assigned'. (**B**) The average RSAF values of two samples are plotted as a function of pre-27S RNAs for each RPL. Error bars are standard deviations. RPLs that are assembled at the cytoplasm or unassigned are colored magenta.

The Ssf1-TAP particle is regarded to represent the earliest state of pre-60S in the nucleolus (22). Notably, a large group of AFs (Mak11, Dbp10, Ssf1, Rrp15, Rrp14, Dbp9, Dbp7, Rrb1, Nug1 and Ybl028c) identified in the Ssf1-TAP particle were absent or extremely weak (RASF < 0.1) in the D6 and 3′ ETS particles (Figure 3A). The plasmid-derived particles appear to be in an eariler state than the Ssf1-TAP particle.

Small amounts of pre-60S AFs have been detected in the Noc4-TAP 90S particle (7) (Figure 3A). These pre-60S AFs may be co-purified with the 90S pre-ribosome through association with the unprocessed 35S pre-rRNA. The pre-60S associated with the Noc4-TAP particle had a protein profile similar to those of the Ssf1-TAP particle and the plasmid-derived pre-60S particles and should be in early assembly stages.

DISCUSSION

Spatiotemporal assembly map of the earliest pre-60S particles

Ribosome assembly study has been traditionally focused on the assembly intermediates after the initial complete pre-ribosome is formed, since these particles are stable and accessible for biochemical purification. On contrast, the intermediates formed during the co-transcriptional assembly process are highly transient and difficult to analyze. Little is known about how the complex structure of large ribosomal subunit is established at the very first stage. To fill the gap, we have derived the first spatiotemporal assembly map for the earliest pre-60S particle by analyzing the composition of RNPs assembled on a series of pre-27S RNAs of increasing length. The map reveals the assembly point of 34 AFs, 30 RPLs and 5S rRNA (Figure 5). The gradual association of

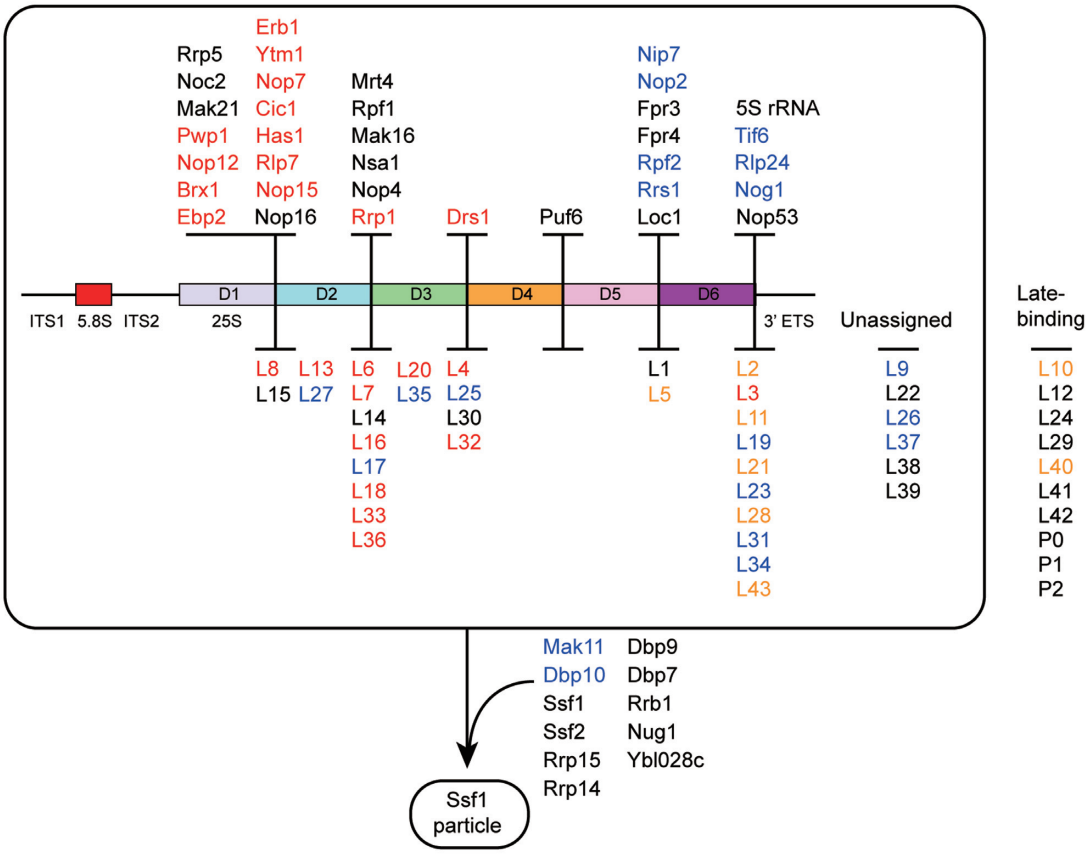

Figure 5. Assembly map of early pre-60S. The AFs and RPLs are placed at their deduced assembly points. A3-factors and B-factors are colored red and blue, respectively. The early, middle, late and other unclassified RPLs are colored red, blue, orange and black, respectively. The rectangular box refers to a pre-60S state before ITS2 processing, which develops into the Ssf1 particle with association of additional AFs.

AFs and RPs with the pre-rRNA fragments strongly supports that the pre-60S is co-transcriptionally assembled on the elongating pre-rRNA and argues against the notion that it is assembled until the entire length of pre-rRNA is transcribed. Combined with the previous studies on 90S (7,8), our study completes the early assembly map for both LSU and SSU in yeast.

For the AFs and RPLs that are present in the determined structures of pre-60S and 60S ribosomes (11–13,47,48), their assembly points are usually consistent with their binding sites. The assembly map also suggests the binding site for 23 out of 34 assigned AFs that have no available structural information at present (Figure 3A), providing insight into the organization of earliest pre-60S particles. Nevertheless, the assembly map does not necessary reflect the actual binding site for AFs and RPLs given that an added RNA segment might directly recruit a protein or induce new binding sites in existing structures. Frequently, the association of a protein is initially weak and then stabilized by extended RNA sequences that may provide additional binding sites. In addition, the Pol II-plasmid system may not fully mimic the Pol I-mediated transcription of pre-rRNA at the nucleolus (49). For example, the processing of Pol II-transcribed pre-rRNA was found to be insensitive to the mutation or depletion of an otherwise essential AF Dim1 (50).

The assembly hierarchy of a few AFs and RPLs was previously deduced by their assembly independence on complete pre-60S particles (38,46,51–54). Our data directly reveal the assembly order of AFs and RPLs on the pre-rRNA in a comprehensive manner and provides the physical basis for their assembly hierarchy. A protein that is required for the association of another protein is normally assembled before or together with the latter protein in the assembly map. For example, Erb1, Ytm1, Nop7, Cic1, Rlp7 and Nop15 are mutually interdependent A3 factors (51) and are co-assembled to the D1 transcript in our map. Pwp1 that is required for assembling the six A3-factors is also co-assembled (54), but Rrp1 that is not required for binding of the six A3-factors is assembled later when the D2 domain is present (51). The assembly order of B-factors is also consistent with their association hierarchy (38).

Sequential assembly of ITS1 and ITS2 processing machineries

One striking observation from our study is that the assembly point of AFs and RPLs was strongly correlated with their function in pre-rRNA processing. The role of many AFs and RPLs has been genetically assigned to specific pre-rRNA processing step (1,2,55). Specifically, 13 AFs and 12 RPLs, known as A3-factors, are required for process-

ing the 27SA3 to 27SB pre-rRNAs (Supplementary Figure S1). The majority of A3-factors are already assembled in the D3 transcript, indicating that the machinery for ITS1 processing is first formed and concentrated on the 5′ half of pre-60S structure. However, at least one essential A3-factor, L3, is not assembled until the 25S region is completely transcribed (Figure 4), thus explaining why ITS1 processing still requires the formation of an entire pre-60S particle. This requirement could serve as a quality control mechanism to ensure that only the pre-rRNA containing full-length 25S rRNA is processed.

Twelve AFs (known as B-factors) are required for C2 cleavage, which splits 27SB into 25.5S and 7S pre-rRNAs (Supplementary Figure S1) (38). In contrast to the early association of A3-factors, all seven B-factors present in the D6 particle are assembled after domains V or VI are transcribed (Figure 3A). The ITS2 processing machinery is incomplete in the D6 particle and additional B-factors are assembled at further downstream stages (Figure 3A). Our data demonstrate that the processing machineries for ITS1 and ITS2 are sequentially recruited by the 5′ and 3′ halves of pre-27S RNA. The assembly order of the ITS1 and ITS2 processing machineries also matches the temporal processing order of ITS1 and ITS2.

Comparison with the hierarchical assembly model of 60S ribosome

An assembly model has been proposed for 60S based on binding hierarchy of RPLs (52). RPLs are grouped into early, middle and late classes for their distinct roles in ITS1 processing, C2 cleavage and 7S processing (2,52). The three classes of RPLs display distinct localization in 60S structure and binding hierarchy. The early RPLs are located at the convex solvent side of 60S structure and required for stable association of most RPLs and AFs. The middle RPLs are distributed around the polypeptide exit tunnel and required for binding of middle and late RPLs. The late RPLs are located at the subunit interface and the CP and required only for assembly of late RPLs. Based on the binding hierarchy and location of RPLs, the solvent interface structure is proposed to form first, followed by the polypeptide exit tunnel, the subunit interface and the CP. Importantly, the hierarchical assembly model and our assembly map describe two different assembly events. Most RPLs are present in the earliest pre-60S particles, but they are not all stably associated (46). The hierarchical assembly model describes the sequential tightening of association of RPLs after formation of the earliest pre-60S particles (52). On contrast, our assembly map depicts earlier assembly events, namely the co-transcriptional binding order of RPLs to pre-rRNA during formation of the earliest pre-60S particles. The assembly maps of bacterial large ribosomal subunits derived from *in vitro* reconstitution and *in vivo* assembly also apply to the full length rRNA (56,57).

Our study shows that the structural core of earliest pre-60S particles, constituted mainly of early RPLs and A3-factors, already begins to assemble in the partially transcribed pre-rRNAs. However, the structural core appears to be incomplete and unstable in the pre-rRNA fragments and is greatly stabilized upon completion of domain VI and assembly of L3, since depletion of L3 would reduce globally the levels of RPLs and AFs in pre-60S (52).

A minor role of the 3′ ETS in early pre-60S assembly

The 3′ ETS contains a stem-loop structure that is cleaved by RNase III Rnt1 during pre-rRNA processing (9). Our data confirm that deletion of the entire 3′ ETS affects the processing of ITS1 and decreases the yield of 25S rRNA (58). Our analysis of the D6 and 3′ ETS particles shows that they share a similar protein composition, suggesting that the 3′ ETS plays a minor role in early pre-60S assembly. The D6 particle contains lower amounts of ITS1-processed pre-rRNAs and late-associating AFs compared to the 3′ ETS particle. The 3′ ETS may regulate the optimal conformation of pre-60S, thereby affecting the rate of ITS1 processing and ribosome maturation.

A novel pre-60S state before ITS2 processing

How pre-60S evolves at the nucleolus is much less understood than its maturation steps at the nucleoplasm and the cytoplasm. The Ssf1-TAP particle is currently the only well-defined nucleolar state of pre-60S (22). By placing the affinity MS2-tag in the ITS2 region, we have selectively purified pre-60S particles arrested before C2 cleavage. The plasmid-derived particles lack ∼10 AFs present in the Ssf1-TAP particle. These AFs appear to be recruited for ITS2 processing, since the Ssf1-TAP particle differs from the plasmid-derived particles by containing ITS2-processed pre-rRNAs. In support of this possibility, among these AFs, Mak11 and Dbp10 are B-factors required for C2 cleavage (59,60). Ssf1 and its closely related paralog Ssf2 regulate the proper timing of C2 cleavage (22). We propose that the fully assembled plasmid-derived particles, excluding those late-associating AFs, represent an earlier state than the Ssf1-TAP particle before C2 cleavage (Figure 5). Association of the Ssf1-specific factors constitutes a discrete step during the nucleolar evolvement of pre-60S.

Comparison of the early assembly pathway of small and large subunits

The SSU is composed of four structurally distinct domains, whereas the LSU contains six domains that are extensively interwoven into a monolithic structure (47,48). Despite their dramatic difference in structural organization, the earliest precursors of both subunits are assembled in a stepwise manner. Such an assembly mode would greatly reduce the complexity of building large RNPs.

Two subunits also exhibit some differences in early assembly in terms of snoRNA involvement and assembly dynamics. The 90S pre-ribosome is associated with U3, U14 and snR30 snoRNAs (7), whereas no snoRNA is involved in LSU assembly in yeast. Consistently, the protein components of box C/D and H/ACA snoRNPs were largely absent in the plasmid-derived pre-60S particles (Supplementary Dataset 1). At the last stage of 90S maturation, a dozen of proteins and U14 and snR30 snoRNAs that bind earlier are released (7). The assembly of pre-60S is less dynamic in terms of AF release. Except for Nop12, which appears to be

released after completion of pre-60S, no other protein exhibits a dramatic reduction in abundance during the course of pre-rRNA elongation.

SUPPLEMENTARY DATA

Supplementary Data are available at NAR Online.

ACKNOWLEDGEMENTS

We thank Gaihong Cai and She Chen at the Proteomics Center of National Institute of Biological Sciences for mass spectrometry analysis, Liman Zhang for help and discussion and Skip Fournier for plasmids.

FUNDING

National Natural Science Foundation of China [31430024, 91540201, 31325007]; Strategic Priority Research Program of the Chinese Academy of Sciences [XDB08010203]; Beijing Municipal Government. Funding for open access charge: National Natural Science Foundation of China [31430024].
Conflict of interest statement. None declared.

REFERENCES

1. Woolford,J.L. Jr and Baserga,S.J. (2013) Ribosome biogenesis in the yeast Saccharomyces cerevisiae. *Genetics*, **195**, 643–681.
2. de la Cruz,J., Karbstein,K. and Woolford,J.L. Jr (2015) Functions of ribosomal proteins in assembly of eukaryotic ribosomes in vivo. *Annu. Rev. Biochem.*, **84**, 93–129.
3. Grandi,P., Rybin,V., Bassler,J., Petfalski,E., Strauss,D., Marzioch,M., Schafer,T., Kuster,B., Tschochner,H., Tollervey,D. *et al.* (2002) 90S pre-ribosomes include the 35S pre-rRNA, the U3 snoRNP, and 40S subunit processing factors but predominantly lack 60S synthesis factors. *Mol. Cell*, **10**, 105–115.
4. Dragon,F., Gallagher,J.E., Compagnone-Post,P.A., Mitchell,B.M., Porwancher,K.A., Wehner,K.A., Wormsley,S., Settlage,R.E., Shabanowitz,J., Osheim,Y. *et al.* (2002) A large nucleolar U3 ribonucleoprotein required for 18S ribosomal RNA biogenesis. *Nature*, **417**, 967–970.
5. Osheim,Y.N., French,S.L., Keck,K.M., Champion,E.A., Spasov,K., Dragon,F., Baserga,S.J. and Beyer,A.L. (2004) Pre-18S ribosomal RNA is structurally compacted into the SSU processome prior to being cleaved from nascent transcripts in Saccharomyces cerevisiae. *Mol. Cell*, **16**, 943–954.
6. Kornprobst,M., Turk,M., Kellner,N., Cheng,J., Flemming,D., Kos-Braun,I., Kos,M., Thoms,M., Berninghausen,O., Beckmann,R. *et al.* (2016) Architecture of the 90S pre-ribosome: a structural view on the birth of the eukaryotic ribosome. *Cell*, **166**, 380–393.
7. Zhang,L., Wu,C., Cai,G., Chen,S. and Ye,K. (2016) Stepwise and dynamic assembly of the earliest precursors of small ribosomal subunits in yeast. *Genes Dev.*, **30**, 718–732.
8. Chaker-Margot,M., Hunziker,M., Barandun,J., Dill,B.D. and Klinge,S. (2015) Stage-specific assembly events of the 6-MDa small-subunit processome initiate eukaryotic ribosome biogenesis. *Nat. Struct. Mol. Biol.*, **22**, 920–923.
9. Kufel,J., Dichtl,B. and Tollervey,D. (1999) Yeast Rnt1p is required for cleavage of the pre-ribosomal RNA in the 3′ ETS but not the 5′ ETS. *RNA*, **5**, 909–917.
10. Elela,S.A., Igel,H. and Ares,M. Jr (1996) RNase III cleaves eukaryotic preribosomal RNA at a U3 snoRNP-dependent site. *Cell*, **85**, 115–124.
11. Wu,S., Tutuncuoglu,B., Yan,K., Brown,H., Zhang,Y., Tan,D., Gamalinda,M., Yuan,Y., Li,Z., Jakovljevic,J. *et al.* (2016) Diverse roles of assembly factors revealed by structures of late nuclear pre-60S ribosomes. *Nature*, **534**, 133–137.
12. Leidig,C., Thoms,M., Holdermann,I., Bradatsch,B., Berninghausen,O., Bange,G., Sinning,I., Hurt,E. and Beckmann,R. (2014) 60S ribosome biogenesis requires rotation of the 5S ribonucleoprotein particle. *Nat. Commun.*, **5**, 3491–3498.
13. Barrio-Garcia,C., Thoms,M., Flemming,D., Kater,L., Berninghausen,O., Bassler,J., Beckmann,R. and Hurt,E. (2016) Architecture of the Rix1-Rea1 checkpoint machinery during pre-60S-ribosome remodeling. *Nat. Struct. Mol. Biol.*, **23**, 37–44.
14. Matsuo,Y., Granneman,S., Thoms,M., Manikas,R.G., Tollervey,D. and Hurt,E. (2014) Coupled GTPase and remodelling ATPase activities form a checkpoint for ribosome export. *Nature*, **505**, 112–116.
15. Weis,F., Giudice,E., Churcher,M., Jin,L., Hilcenko,C., Wong,C.C., Traynor,D., Kay,R.R. and Warren,A.J. (2015) Mechanism of eIF6 release from the nascent 60S ribosomal subunit. *Nat. Struct. Mol. Biol.*, **22**, 914–919.
16. Greber,B.J., Gerhardy,S., Leitner,A., Leibundgut,M., Salem,M., Boehringer,D., Leulliot,N., Aebersold,R., Panse,V.G. and Ban,N. (2015) Insertion of the biogenesis factor Rei1 probes the ribosomal tunnel during 60S maturation. *Cell*, **164**, 91–102.
17. Panse,V.G. and Johnson,A.W. (2010) Maturation of eukaryotic ribosomes: acquisition of functionality. *Trends Biochem. Sci.*, **35**, 260–266.
18. Liang,W.Q. and Fournier,M.J. (1997) Synthesis of functional eukaryotic ribosomal RNAs in trans: development of a novel in vivo rDNA system for dissecting ribosome biogenesis. *Proc. Natl. Acad. Sci. U.S.A.*, **94**, 2864–2868.
19. Erijman,A., Dantes,A., Bernheim,R., Shifman,J.M. and Peleg,Y. (2011) Transfer-PCR (TPCR): a highway for DNA cloning and protein engineering. *J. Struct. Biol.*, **175**, 171–177.
20. Nissan,T.A., Bassler,J., Petfalski,E., Tollervey,D. and Hurt,E. (2002) 60S pre-ribosome formation viewed from assembly in the nucleolus until export to the cytoplasm. *EMBO J.*, **21**, 5539–5547.
21. Rigaut,G., Shevchenko,A., Rutz,B., Wilm,M., Mann,M. and Seraphin,B. (1999) A generic protein purification method for protein complex characterization and proteome exploration. *Nat. Biotechnol.*, **17**, 1030–1032.
22. Fatica,A., Cronshaw,A.D., Dlakic,M. and Tollervey,D. (2002) Ssf1p prevents premature processing of an early pre-60S ribosomal particle. *Mol. Cell*, **9**, 341–351.
23. Nissan,T.A., Galani,K., Maco,B., Tollervey,D., Aebi,U. and Hurt,E. (2004) A pre-ribosome with a tadpole-like structure functions in ATP-dependent maturation of 60S subunits. *Mol. Cell*, **15**, 295–301.
24. Bradatsch,B., Leidig,C., Granneman,S., Gnadig,M., Tollervey,D., Bottcher,B., Beckmann,R. and Hurt,E. (2012) Structure of the pre-60S ribosomal subunit with nuclear export factor Arx1 bound at the exit tunnel. *Nat. Struct. Mol. Biol.*, **19**, 1234–1241.
25. Zhang,J., Harnpicharnchai,P., Jakovljevic,J., Tang,L., Guo,Y., Oeffinger,M., Rout,M.P., Hiley,S.L., Hughes,T. and Woolford,J.L. Jr (2007) Assembly factors Rpf2 and Rrs1 recruit 5S rRNA and ribosomal proteins rpL5 and rpL11 into nascent ribosomes. *Genes Dev.*, **21**, 2580–2592.
26. Hierlmeier,T., Merl,J., Sauert,M., Perez-Fernandez,J., Schultz,P., Bruckmann,A., Hamperl,S., Ohmayer,U., Rachel,R., Jacob,A. *et al.* (2013) Rrp5p, Noc1p and Noc2p form a protein module which is part of early large ribosomal subunit precursors in S. cerevisiae. *Nucleic Acids Res.*, **41**, 1191–1210.
27. Krogan,N.J., Peng,W.T., Cagney,G., Robinson,M.D., Haw,R., Zhong,G., Guo,X., Zhang,X., Canadien,V., Richards,D.P. *et al.* (2004) High-definition macromolecular composition of yeast RNA-processing complexes. *Mol. Cell*, **13**, 225–239.
28. Zhang,W., Morris,Q.D., Chang,R., Shai,O., Bakowski,M.A., Mitsakakis,N., Mohammad,N., Robinson,M.D., Zirngibl,R., Somogyi,E. *et al.* (2004) The functional landscape of mouse gene expression. *J. Biol.*, **3**, 21.
29. Shimoji,K., Jakovljevic,J., Tsuchihashi,K., Umeki,Y., Wan,K., Kawasaki,S., Talkish,J., Woolford,J.L. Jr and Mizuta,K. (2012) Ebp2 and Brx1 function cooperatively in 60S ribosomal subunit assembly in Saccharomyces cerevisiae. *Nucleic Acids Res.*, **40**, 4574–4588.
30. Miles,T.D., Jakovljevic,J., Horsey,E.W., Harnpicharnchai,P., Tang,L. and Woolford,J.L. Jr (2005) Ytm1, Nop7, and Erb1 form a complex necessary for maturation of yeast 66S preribosomes. *Mol. Cell. Biol.*, **25**, 10419–10432.

31. Holzel,M., Rohrmoser,M., Schlee,M., Grimm,T., Harasim,T., Malamoussi,A., Gruber-Eber,A., Kremmer,E., Hiddemann,W., Bornkamm,G.W. *et al.* (2005) Mammalian WDR12 is a novel member of the Pes1-Bop1 complex and is required for ribosome biogenesis and cell proliferation. *J. Cell Biol.*, **170**, 367–378.
32. Lapik,Y.R., Fernandes,C.J., Lau,L.F. and Pestov,D.G. (2004) Physical and functional interaction between Pes1 and Bop1 in mammalian ribosome biogenesis. *Mol. Cell*, **15**, 17–29.
33. Dembowski,J.A., Ramesh,M., McManus,C.J. and Woolford,J.L. Jr (2013) Identification of the binding site of Rlp7 on assembling 60S ribosomal subunits in Saccharomyces cerevisiae. *RNA*, **19**, 1639–1647.
34. Granneman,S., Petfalski,E. and Tollervey,D. (2011) A cluster of ribosome synthesis factors regulate pre-rRNA folding and 5.8S rRNA maturation by the Rat1 exonuclease. *EMBO J.*, **30**, 4006–4019.
35. Lebaron,S., Segerstolpe,A., French,S.L., Dudnakova,T., de Lima Alves,F., Granneman,S., Rappsilber,J., Beyer,A.L., Wieslander,L. and Tollervey,D. (2013) Rrp5 binding at multiple sites coordinates pre-rRNA processing and assembly. *Mol. Cell*, **52**, 707–719.
36. Qiu,C., McCann,K.L., Wine,R.N., Baserga,S.J. and Hall,T.M. (2014) A divergent Pumilio repeat protein family for pre-rRNA processing and mRNA localization. *Proc. Natl. Acad. Sci. U.S.A.*, **111**, 18554–18559.
37. Sharma,S., Yang,J., Watzinger,P., Kotter,P. and Entian,K.D. (2013) Yeast Nop2 and Rcm1 methylate C2870 and C2278 of the 25S rRNA, respectively. *Nucleic Acids Res.*, **41**, 9062–9076.
38. Talkish,J., Zhang,J., Jakovljevic,J., Horsey,E.W. and Woolford,J.L. Jr (2012) Hierarchical recruitment into nascent ribosomes of assembly factors required for 27SB pre-rRNA processing in Saccharomyces cerevisiae. *Nucleic Acids Res.*, **40**, 8646–8661.
39. Madru,C., Lebaron,S., Blaud,M., Delbos,L., Pipoli,J., Pasmant,E., Rety,S. and Leulliot,N. (2015) Chaperoning 5S RNA assembly. *Genes Dev.*, **29**, 1432–1446.
40. Kharde,S., Calvino,F.R., Gumiero,A., Wild,K. and Sinning,I. (2015) The structure of Rpf2-Rrs1 explains its role in ribosome biogenesis. *Nucleic Acids Res.*, **43**, 7083–7095.
41. Asano,N., Kato,K., Nakamura,A., Komoda,K., Tanaka,I. and Yao,M. (2015) Structural and functional analysis of the Rpf2-Rrs1 complex in ribosome biogenesis. *Nucleic Acids Res.*, **43**, 4746–4757.
42. Thoms,M., Thomson,E., Bassler,J., Gnadig,M., Griesel,S. and Hurt,E. (2015) The exosome is recruited to RNA substrates through specific adaptor proteins. *Cell*, **162**, 1029–1038.
43. Thomson,E. and Tollervey,D. (2005) Nop53p is required for late 60S ribosome subunit maturation and nuclear export in yeast. *RNA*, **11**, 1215–1224.
44. Sydorskyy,Y., Dilworth,D.J., Halloran,B., Yi,E.C., Makhnevych,T., Wozniak,R.W. and Aitchison,J.D. (2005) Nop53p is a novel nucleolar 60S ribosomal subunit biogenesis protein. *Biochem. J.*, **388**, 819–826.
45. Granato,D.C., Gonzales,F.A., Luz,J.S., Cassiola,F., Machado-Santelli,G.M. and Oliveira,C.C. (2005) Nop53p, an essential nucleolar protein that interacts with Nop17p and Nip7p, is required for pre-rRNA processing in Saccharomyces cerevisiae. *FEBS J.*, **272**, 4450–4463.
46. Ohmayer,U., Gamalinda,M., Sauert,M., Ossowski,J., Poll,G., Linnemann,J., Hierlmeier,T., Perez-Fernandez,J., Kumcuoglu,B., Leger-Silvestre,I. *et al.* (2013) Studies on the assembly characteristics of large subunit ribosomal proteins in S. cerevisae. *PLoS One*, **8**, e68412.
47. Klinge,S., Voigts-Hoffmann,F., Leibundgut,M., Arpagaus,S. and Ban,N. (2011) Crystal structure of the eukaryotic 60S ribosomal subunit in complex with initiation factor 6. *Science*, **334**, 941–948.
48. Ben-Shem,A., Garreau de Loubresse,N., Melnikov,S., Jenner,L., Yusupova,G. and Yusupov,M. (2011) The structure of the eukaryotic ribosome at 3.0 A resolution. *Science*, **334**, 1524–1529.
49. Nogi,Y., Yano,R. and Nomura,M. (1991) Synthesis of large rRNAs by RNA polymerase II in mutants of Saccharomyces cerevisiae defective in RNA polymerase I. *Proc. Natl. Acad. Sci. U.S.A.*, **88**, 3962–3966.
50. Lafontaine,D.L., Preiss,T. and Tollervey,D. (1998) Yeast 18S rRNA dimethylase Dim1p: a quality control mechanism in ribosome synthesis? *Mol. Cell. Biol.*, **18**, 2360–2370.
51. Sahasranaman,A., Dembowski,J., Strahler,J., Andrews,P., Maddock,J. and Woolford,J.L. Jr (2011) Assembly of Saccharomyces cerevisiae 60S ribosomal subunits: role of factors required for 27S pre-rRNA processing. *EMBO J.*, **30**, 4020–4032.
52. Gamalinda,M., Ohmayer,U., Jakovljevic,J., Kumcuoglu,B., Woolford,J., Mbom,B., Lin,L. and Woolford,J.L. Jr (2014) A hierarchical model for assembly of eukaryotic 60S ribosomal subunit domains. *Genes Dev.*, **28**, 198–210.
53. Jakovljevic,J., Ohmayer,U., Gamalinda,M., Talkish,J., Alexander,L., Linnemann,J., Milkereit,P. and Woolford,J.L. Jr (2012) Ribosomal proteins L7 and L8 function in concert with six A3 assembly factors to propagate assembly of domains I and II of 25S rRNA in yeast 60S ribosomal subunits. *RNA*, **18**, 1805–1822.
54. Talkish,J., Campbell,I.W., Sahasranaman,A., Jakovljevic,J. and Woolford,J.L. Jr (2014) Ribosome assembly factors Pwp1 and Nop12 are important for folding of 5.8S rRNA during ribosome biogenesis in Saccharomyces cerevisiae. *Mol. Cell. Biol.*, **34**, 1863–1877.
55. Poll,G., Braun,T., Jakovljevic,J., Neueder,A., Jakob,S., Woolford,J.L. Jr, Tschochner,H. and Milkereit,P. (2009) rRNA maturation in yeast cells depleted of large ribosomal subunit proteins. *PLoS One*, **4**, e8249.
56. Rohl,R. and Nierhaus,K.H. (1982) Assembly map of the large subunit (50S) of Escherichia coli ribosomes. *Proc. Natl. Acad. Sci. U.S.A.*, **79**, 729–733.
57. Chen,S.S. and Williamson,J.R. (2013) Characterization of the ribosome biogenesis landscape in E. coli using quantitative mass spectrometry. *J. Mol. Biol.*, **425**, 767–779.
58. Allmang,C. and Tollervey,D. (1998) The role of the 3′ external transcribed spacer in yeast pre-rRNA processing. *J. Mol. Biol.*, **278**, 67–78.
59. Burger,F., Daugeron,M.C. and Linder,P. (2000) Dbp10p, a putative RNA helicase from Saccharomyces cerevisiae, is required for ribosome biogenesis. *Nucleic Acids Res.*, **28**, 2315–2323.
60. Saveanu,C., Rousselle,J.C., Lenormand,P., Namane,A., Jacquier,A. and Fromont-Racine,M. (2007) The p21-activated protein kinase inhibitor Skb15 and its budding yeast homologue are 60S ribosome assembly factors. *Mol. Cell. Biol.*, **27**, 2897–2909.